Article

Structure of Ethene Adsorption Sites on Supported Metal Catalysts from in Situ XANES Analysis

Eveline Bus, David E. Ramaker, and Jeroen A. van Bokhoven

J. Am. Chem. Soc., **2007**, 129 (26), 8094-8102• DOI: 10.1021/ja0689233 • Publication Date (Web): 12 June 2007

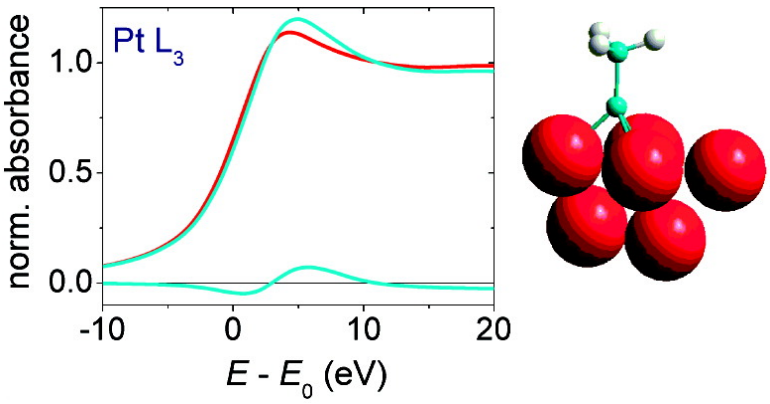

More About This Article

Additional resources and features associated with this article are available within the HTML version:

- Supporting Information
- Links to the 1 articles that cite this article, as of the time of this article download
- Access to high resolution figures
- Links to articles and content related to this article
- Copyright permission to reproduce figures and/or text from this article

View the Full Text HTML

J|A|C|S
ARTICLES
Published on Web 06/12/2007

Structure of Ethene Adsorption Sites on Supported Metal Catalysts from in Situ XANES Analysis

Eveline Bus,[†] David E. Ramaker,[‡] and Jeroen A. van Bokhoven*

Contribution from the Institute for Chemical and Bioengineering, ETH Zurich, 8093 Zurich, Switzerland, and Department of Chemistry and Materials Science Institute, George Washington University, Washington, DC 20052

Received December 13, 2006; E-mail: j.a.vanbokhoven@chem.ethz.ch

Abstract: The structures of the catalytically active sites in supported metal catalysts are a long sought after goal. In this study, XAS has been used to establish these structures. The ethene-induced changes in the XAS spectra as a function of temperature and pressure were correlated to changes in the adsorption mode of the hydrocarbon. At low temperature, ethene was adsorbed in on-top (π) and bridged (di-σ) sites on small platinum clusters. Below room temperature, the adsorbed ethene was dehydrogenated to an ethylidyne species, which was adsorbed in threefold Pt sites. On larger clusters the dehydrogenation proceeded at higher temperature indicating a different reactivity. EXAFS results showed that changes in the geometrical structures were mainly due to (co)adsorbed hydrogen. Our results for platinum agree with those obtained using other techniques proving that detailed shape analysis of the L_3 edge XANES is a practical tool to determine the structure of the sites that are involved in bonding to reactants and intermediates. Application to gold and alloy catalysts showed that ethene induced a significant change in the electronic structure of gold nanoclusters that could be interpreted as ethene adsorbed on top of single gold atoms or in bridged sites. Ethene adsorbed on both platinum and gold in the bimetallic clusters.

Introduction

Supported metal catalysts activate hydrocarbon molecules and are therefore widely applied in the chemical industry. The adsorption modes of the reactants, intermediates, and products affect their activity and selectivity. These adsorbates occupy a specific site on the metal surface, which depends on the type of metal, the cluster size, the metal oxide support, and alloying. Revealing the structures of the adsorption sites provides insight into the mechanisms of how small metal clusters activate hydrocarbon molecules, which, ultimately, enable tuning of the catalytic performance. Since ethene is the smallest molecule containing a carbon−carbon double bond, the adsorption of ethene on metal surfaces is an often-used model reaction.[1−5] At low temperature, ethene adsorbs molecularly on the Pt(111) surface, forming a π-bonded surface species.[1] At 240 K and 10^{-4} Pa, ethene adsorbs in the di-σ mode, in bridged sites. Upon heating to 270 K, a CH_3CH intermediate is formed that is dehydrogenated to ethylidyne (CH_3C), which is adsorbed in threefold metal sites.[2,3] Such information has come from vibrational spectroscopy studies under UHV conditions on single crystals,[1−3] and theoretical studies that have provided further insight into the bonding of reactants and intermediates on metal surfaces.[6−8] However, the sites that are involved in hydrocarbon conversions are often unidentified for molecules larger than ethene,[3] and the structures of the active sites on supported metal catalysts remain largely unknown. Our aim is the selective detection of these structures on small metal clusters in powder catalysts, i.e., the active components in industrial catalysts. As industrial conditions deviate from UHV conditions and can even reach tens or hundreds of bars, and the hydrocarbon chemistry on metal surfaces varies with partial pressure of the reactants,[3] and a technique that can be applied under catalytically relevant conditions is required. Recent developments have shown that the adsorption sites of various atoms and molecules on metal clusters can be determined with X-ray absorption spectroscopy (XAS), a technique that can be applied under high pressures and temperatures. The positioning of hydrogen atoms on Pt as a function of coverage has been determined by examining spectral changes in the X-ray absorption near-edge structures (XANES or delta XANES) along with the aid of FEFF8 calculations.[9−13] Similarly, Pt−O and Pt−OH interactions in

[†] ETH Zurich.
[‡] George Washington University.

(1) Cassuto, A.; Kiss, J.; White, J. M. *Surf. Sci.* **1991**, *255*, 289.
(2) Land, T. A.; Michely, T.; Behm, R. J.; Hemminger, J. C.; Comsa, G. *J. Chem. Phys.* **1992**, *97*, 6774.
(3) Somorjai, G. A.; Marsh, A. L. *Phil. Trans. R. Soc. London, Ser. A* **2005**, *363*, 879.
(4) Alexeev, O. S.; Li, F.; Amiridis, M. D.; Gates, B. C. *J. Phys. Chem. B* **2005**, *109*, 2338.
(5) Argo, A. M.; Odzak, J. F.; Lai, F. S.; Gates, B. C. *Nature* **2002**, *415*, 623.
(6) Delbecq, F.; Sautet, P. *J. Catal* **1995**, *152*, 217.
(7) Morin, C.; Simon, D.; Sautet, P. *J. Phys. Chem. B* **2004**, *108*, 12084.
(8) Loffreda, D.; Delbecq, F.; Vigné, F.; Sautet, P. *J. Am. Chem. Soc.* **2006**, *128*, 1316.
(9) Ramaker, D. E.; Mojet, B. L.; Oostenbrink, M. T. G.; Miller, J. T.; Koningsberger, D. C. *Phys. Chem. Chem. Phys.* **1999**, *1*, 2293.
(10) Ankudinov, A. L.; Rehr, J. J.; Low, J.; Bare, S. R. *Phys. Rev. Lett.* **2001**, *86*, 1642.
(11) Ramaker, D. E.; Koningsberger, D. C. *Phys. Rev. Lett.* **2002**, *89*, 139701.
(12) Teliska, M.; O'Grady, W. E.; Ramaker, D. E. *J. Phys. Chem. B* **2004**, *108*, 2333.
(13) Oudenhuijzen, M. K.; van Bokhoven, J. A.; Miller, J. T.; Ramaker, D. E.; Koningsberger, D. C. *J. Am. Chem. Soc.* **2005**, *127*, 1530.

10.1021/ja0689233 CCC: $37.00

an electrochemical cell and in a working fuel cell have been examined,[14,15] and the difference spectra induced by the binding of CO on gold and platinum clusters have been described previously.[16,17] Nearly quantitative agreement between theoretical and experimental high-energy resolution XANES spectra was found before and after the adsorption of CO on small Pt clusters.[18] The XANES also provides electronic information such as the empty density of states. At the same time, the extended X-ray absorption fine structure (EXAFS) provides the local metal structure such as metal−metal bond lengths and number and type of neighbors. Previous FEFF8 calculations have shown that the white-line intensity stays approximately constant with cluster size for 3D close-packed and polytetrahedral clusters. The cluster geometry, however, does affect the white line as the 2D close-packed systems exhibit more intense white lines than the 3D clusters.[19] Fortunately, the changes in the white line from these geometry changes differ from those induced by adsorbates on small clusters enabling the distinction between geometry-[19] and adsorbate-induced changes.

Here, the binding sites of ethene on noble metal nanoclusters (Pt, Au, and PtAu) under various pressures and temperatures are established using the delta XANES technique on the Pt and Au L edges. Platinum catalysts that are widely used in industry were studied first, showing the ability of in situ XAS to detect the structure of the adsorbate sites on supported metal catalysts that activate hydrocarbons. The support- and cluster-size effects are discussed. Recently, it was found that gold is also active in hydrocarbon reforming.[20−23] Since the structure of the active sites in the supported gold catalysts is a matter of debate, we studied the adsorption sites of ethene on Au/Al_2O_3. Furthermore, the catalytic activity of platinum alloyed with gold is distinctly different from that of the pure metals. This different catalytic activity can originate from geometric and electronic effects, inducing different modes of adsorption as experimentally observed.[24,25] Gold is often considered an inactive additive in these alloy catalysts. We show that both platinum and gold interact with ethene in PtAu-alloy clusters.

Experimental Section

The 2 wt % Pt/Al_2O_3 was prepared by incipient-wetness impregnation of γ-Al_2O_3 (Condea, 0.51 mL/g, 230 m^2/g) with an aqueous solution of tetraammine platinum nitrate (PTA) and calcination at 673 K. The 2 wt % $Pt/SiO_2-Al_2O_3$ and 1 wt % Pt/SiO_2 were prepared by adding an aqueous solution of PTA to a slurry of $SiO_2-Al_2O_3$ (Davison 135) or SiO_2 (Davison 644, 1 mL/g, 290 m^2/g), respectively, in an NH_4OH solution with a pH of 10. After filtering and washing, $Pt/SiO_2-Al_2O_3$ was prereduced in hydrogen at 523 K and Pt/SiO_2 at 473 or 873 K. Hydrogen uptake measurements of the Pt catalysts were done at 300 K under static volumetric conditions with a Micromeritics ASAP 2010 apparatus. The H/Pt ratio is the ratio of the number of adsorbed H atoms to the total number of Pt atoms, the former obtained by extrapolating the linear high-pressure part of the first adsorption isotherm to zero pressure. The 0.5 wt % Au/Al_2O_3 was prepared by incipient-wetness impregnation of γ-Al_2O_3 with an aqueous solution of $HAuCl_4$. Stirring the powder in water at 343 K, and maintaining a pH of 8 using NaOH, removed chlorine.[26] $PtAu/SiO_2$ was prepared by adding $Pt_2Au_4(C{\equiv}CBu^t)_8$ to a slurry of SiO_2 (Merck 60, 0.74 mL/g, 460 m^2/g) in hexane, filtering, and drying.[27,28] The metal loading was 2 wt % Au and 1 wt % Pt. Metallic PtAu clusters were obtained after calcination at 573 K and reduction at 473 K.

The XAS experiments were performed at beam line X1 of HASYLAB (Hamburg, Germany) and at the DUBBLE station (BM26A) at the ESRF (Grenoble, France). At beam line X1 the double-crystal monochromator was equipped with Si(111) crystals that were detuned to 70% of the intensity to remove higher harmonics. At the DUBBLE station, the double-crystal monochromator was followed by two vertically focusing Pt- and Si-coated mirrors to reject higher harmonics. All spectra were recorded in transmission mode using ionization chambers for detection. The sample was pressed into a self-supporting wafer and placed in a stainless-steel in situ cell[29] that was connected to a gas-flow system, temperature controller, liquid-nitrogen tank, and turbo molecular vacuum pump. Prior to the experiments, the catalysts were reduced in situ in pure hydrogen. Pt/Al_2O_3 was reduced at 723 K, $Pt/SiO_2-Al_2O_3$ at 573 K, and Pt/SiO_2, Au/Al_2O_3, and $PtAu/SiO_2$ at 473 K. The chemisorbed hydrogen was removed by evacuation ($<10^{-3}$ Pa) at 473 K or higher, and L edge spectra were collected at several temperatures. Ethene was adsorbed at 77 or 300 K by passing an ethene in helium or ethene flow through the cell. L edge spectra of the catalysts in static or flowing ethene were collected at the adsorption temperature and after heating with 5 K/min to 300, 373, or 473 K. L_3 edge spectra for Pt/Al_2O_3 were collected while removing ethene by heating under vacuum. L edge spectra for Pt/Al_2O_3 and Pt/SiO_2 were also collected in hydrogen and in a gas mixture of ethene and hydrogen.

XAS data analysis was carried out using the XDAP software package.[30] The absorption data were background subtracted by means of standard procedures[31] and normalized on the height of the edge step at 50 eV above the edge. EXAFS multiple-shell fitting was performed in R space using k weightings of 1−3. It was not necessary to include multiple-scattering paths. Higher-order cumulants were included, and when fitting both a metal−metal and a metal−light scatterer shell, $E_{0,\text{light scatterer}}$ was kept equal to zero and $C_{4,\text{light scatterer}}$ equal to $C_{4,\text{metal}}$.[32] Experimentally calibrated theoretical references obtained with the FEFF8 code[33] were used to obtain S_0^2, F, and δ.

Alignment of the normalized XANES spectra, to remove initial-state core level shifts and final-state screening effects, was done by setting the energy of the point in the L_2 edges having an intensity of 0.4 to zero.[9,34] The first derivative of the L_3 EXAFS oscillations between 50 and 120 eV above the edge was then aligned on the first derivative

(14) Teliska, M.; O'Grady, W. E.; Ramaker, D. E. *J. Phys. Chem. B* **2005**, *109*, 8076.
(15) Roth, C.; Benker, N.; Buhrmester, T.; Mazurek, M.; Loster, M.; Fuess, H.; Koningsberger, D. C.; Ramaker, D. E. *J. Am. Chem. Soc.* **2005**, *127*, 14607.
(16) Weiher, N.; Bus, E.; Delannoy, L.; Louis, C.; Ramaker, D. E.; Miller, J. T.; van Bokhoven, J. A. *J. Catal.* **2006**, *240*, 100.
(17) Scott, F. J.; Mukerjee, S.; Ramaker, D. E. *J. Electrochem. Soc.* **2007**, *154*, A396.
(18) Safonova, O. V.; Tromp, M.; van Bokhoven, J. A.; de Groot, F. M. F.; Evans, F.; Glatzel, P. *J. Phys. Chem B* **2006**, *110*, 16162.
(19) Ankudinov, A. L.; Rehr, J. J.; Low, J. J.; Bare, S. R. *J. Chem. Phys.* **2002**, *116*, 1911.
(20) Haruta, M. *Catal. Today* **1997**, *36*, 153.
(21) Valden, M.; Lai, X.; Goodman, D. W. *Science* **1998**, *281*, 1647.
(22) Sivadinarayana, C.; Choudhary, T. V.; Daemen, L. L.; Eckert, J.; Goodman, D. W. *J. Am. Chem. Soc.* **2004**, *126*, 38.
(23) Bus, E.; Prins, R.; van Bokhoven, J. A. *Catal. Commun.* **2007**, *8*, 1397.
(24) Yeates, R. C.; Somorjai, G. A. *J. Catal.* **1987**, *103*, 208.
(25) Chandler, B. D.; Schabel, A. B.; Pignolet, L. H. *J. Phys. Chem. B* **2001**, *105*, 149.
(26) Yang, J. Y.; Henao, J. D.; Costello, C.; Kung, M. C.; Kung, H. H.; Miller, J. T.; Kropf, A. J.; Kim, J.-G.; Regalbuto, J. R.; Bore, M. T.; Pham, H. N.; Datye, A. K.; Laeger, J. D.; Kharas, K. *Appl. Catal., A* **2005**, *291*, 73.
(27) Espinet, P.; Fornies, J.; Martinez, F.; Tomas, M. *J. Chem. Soc., Dalton Trans.* **1990**, 791.
(28) Chandler, B. D.; Schabel, A. B.; Blanford, C. F.; Pignolet, L. H. *J. Catal.* **1999**, *187*, 367.
(29) Vaarkamp, M.; Mojet, B. L.; Kappers, M. J.; Miller, J. T.; Koningsberger, D. C. *J. Phys. Chem.* **1995**, *99*, 16067.
(30) Vaarkamp, M.; Linders, J. C.; Koningsberger, D. C. *Physica B* **1995**, *208*, 159.
(31) Koningsberger, D. C.; Mojet, B. L.; van Dorssen, G. E.; Ramaker, D. E. *Top. Catal.* **2000**, *10*, 143.
(32) Bus, E.; Miller, J. T.; Kropf, A. J.; Prins, R.; van Bokhoven, J. A. *Phys. Chem. Chem. Phys.* **2006**, *8*, 3248.
(33) Zabinsky, S. I.; Rehr, J. J.; Ankudinov, A.; Albers, R. C.; Eller, M. J. *Phys. Rev. B* **1995**, *52*, 2995.
(34) Bus, E.; Miller, J. T.; van Bokhoven, J. A. *J. Phys. Chem. B* **2005**, *109*, 14581.

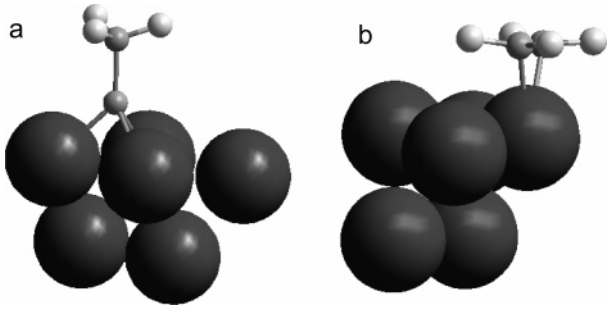

Figure 1. (a) Ethylidyne and (b) π-bonded ethene on a Pt_6 cluster, as used in the FEFF8 calculations. Pt (dark-gray spheres), C (gray spheres), and H (white spheres).

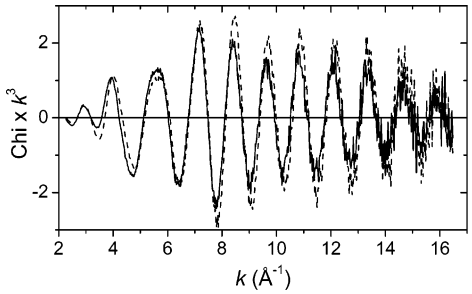

Figure 2. k^3-weighted EXAFS function for Pt/Al_2O_3 under vacuum (---) and in ethene atmosphere (—) at 300 K.

of the L_2 EXAFS oscillations measured under the same conditions by means of the least-squares method. XANES difference spectra ($\Delta\mu$) were extracted by subtracting the L_3 edge collected under vacuum from that collected in the gas atmosphere, mostly at the same temperature. To interpret the experimental $\Delta\mu$ spectra, self-consistent full multiple-scattering calculations of the Pt and Au L_3 XANES were performed with the FEFF8 code. A Hedin−Lundqvist potential and the L_3 XANES, LDOS, NOHOLE, SCF, and FMS cards were used. A cluster consisting of six metal atoms was used (Figure 1). Four atoms form the base and are placed in a square arrangement, for example the four atoms in front in Figure 1a. Two additional atoms are positioned below this plane. On a cluster like this, all different adsorption sites, such as hcp, fcc, bridged, and on-top are present.[35] The atom coordinates of ethene in the adsorption modes π, di-σ, and ethylidyne (Figure 1) were optimized using force-field calculations (MM3 calculations in Hyperchem: Hypercube, Inc., Gainesville, FL). So-called spectral $\Delta\mu$ signatures of the different adsorbate sites were calculated by taking the difference between the spectra for the cluster with ethene and that for the bare metal cluster.

Results

Platinum Catalysts. Figure 2 shows the EXAFS function for Pt/Al_2O_3 at 300 K under vacuum and in ethene atmosphere. The data quality was good up to 16 $Å^{-1}$, and good fits were obtained. The resultant parameters for all Pt catalysts under various conditions are given in Table 1. The first coordination shell was fit; no higher shells were present. The Pt−Pt coordination number (N_{Pt-Pt}) for Pt/Al_2O_3 and $Pt/SiO_2-Al_2O_3$ under vacuum was around 6. Thus, the cluster size was 0.8 nm, in agreement with the measured H/Pt ratios above 1.[36,37] Pt/SiO_2 reduced at 473 K (Pt/SiO_2-473) had an N_{Pt-Pt} of 5.1, corresponding to a cluster size of 0.6 nm. In these small clusters, the Pt−Pt distance (R_{Pt-Pt}) under vacuum after the removal of hydrogen was 2.68−2.70 Å, which shows the contraction of the metal−metal distance typical of small clusters.[38] A contribution of a light scatterer with an N of 0.1−0.4 was observed at ca. 2 Å, which is ascribed to an oxygen atom of the support. Pt/SiO_2 that was prereduced at 873 K (Pt/SiO_2-873) had an H/Pt ratio of 0.28. N_{Pt-Pt} was around 9, R_{Pt-Pt} was 2.75 Å, and the contribution of support oxygen was too low to be detected. Thus, these platinum clusters were much larger with a bulklike structure.

Upon addition of hydrogen to Pt/Al_2O_3 and Pt/SiO_2-473, N_{Pt-Pt} increased to 6.7 and R_{Pt-Pt} increased by 0.04 to 0.06 Å, caused by the electron-withdrawing properties of the hydrogen atoms.[39] For all Pt catalysts, addition of ethene resulted in similar Pt−Pt coordination numbers and distances like those found for the bare metal clusters, suggesting that the structure of the metal clusters is insensitive to the adsorption of ethene. Upon heating in ethene atmosphere, R_{Pt-Pt} for the small Pt clusters increased. Analysis of the difference between the EXAFS with and without ethene at 300 K indicated that the contribution of the light scatterer increased for the catalysts with small clusters. In addition to contributions from the support oxygens, a contribution of carbon from adsorbed ethene was detected that decreased upon heating. However, the small intensity of the light-scatterer contribution compared to the Pt−Pt scattering did not allow a more accurate analysis.

Addition of ethene to the Pt catalysts induced an effect in the XANES at all three L edges (Figure 3). The Pt L_3 edges for Pt/Al_2O_3 and $Pt/SiO_2-Al_2O_3$ shifted to higher energy, and the white line had an enhanced intensity after the adsorption of ethene while the intensity decreased in the region 10−40 eV above the edge (Figure 3a,d). The L_3 edges in 25 kPa partial pressure of ethene and in pure ethene did not differ significantly; at lower partial pressure the white-line intensity was slightly lower, and the positive edge shift was smaller. The changes in the edge upon addition of the ethene/He gas mixture were not due to air that could have unintentionally entered the in situ XAS cell, because upon oxidation an increase in R_{Pt-Pt} and a decrease in N_{Pt-Pt} would have been observed. The intensity in the white-line region of the L_2 edge increased upon ethene adsorption, and above 10 eV the intensity decreased (Figure 3b). These changes are similar to those present in the L_3 edge, since both edges probe the empty d DOS. The L_1 edge probes the p band. The Pt L_1 edge shifted slightly to higher energy upon ethene adsorption (Figure 3c). Its intensity increased between 13 and 33 eV and decreased between 33 and 50 eV above the edge. These changes in the EXAFS region are due to the changes in the geometric structure, mainly the addition of a Pt−C contribution. Subsequent evacuation at 300 K resulted in a further change in the L edge spectra. The effect of ethene on the platinum clusters was reversible, and at 723 K all ethene was removed.

To emphasize the changes in the spectra, L_3 $\Delta\mu$ difference spectra were calculated, with the spectrum of the bare metal measured at the same temperature used as reference. These $\Delta\mu$ difference spectra for Pt/Al_2O_3 at 77, 300, and 473 K are shown

(35) Janin, E.; von Schenck, H.; Göthelid, M.; Karlsson, U. O.; Svensson, M. *Phys. Rev. B* **2000**, *61*, 13144.
(36) de Graaf, J.; van Dillen, A. J.; de Jong, K. P.; Koningsberger, D. C. *J. Catal.* **2001**, *203*, 307.
(37) Kip, B. J.; Duivenvoorden, F. B. M.; Koningsberger, D. C.; Prins, R. *J. Catal.* **1987**, *105*, 26.
(38) Delley, B.; Ellis, D. E.; Freeman, A. J.; Baerends, E. J.; Post, D. *Phys. Rev. B* **1983**, *27*, 2132.
(39) Sanchez Marcos, E.; Jansen, A. P. J.; van Santen, R. A. *Chem. Phys. Lett.* **1990**, *167*, 399.

Table 1. Structural Parameters of the Platinum Catalysts under Various Conditions as Determined by EXAFS Fitting of the Pt L_3 Edges[a,b] and the Measured H/Pt Ratios in Brackets[c]

			Pt–Pt shell				Pt–light scatterer shell		
catalyst	T (K)	atmosphere	N	$\Delta\sigma^2$ (10^{-4} Å^2)	R (Å)	ΔE_0 (eV)	N	$\Delta\sigma^2$ (10^{-4} Å^2)	R (Å)
Pt/Al_2O_3	77	vacuum	5.7	36	2.68	0.9	0.4	−13	2.0
(1.51)		ethene	5.9	27	2.68	2.8	0.6	27	2.0
	300	vacuum	5.6	43	2.68	1.2	0.4	39	2.0
		hydrogen	6.7	52	2.72	1.3	0.4	0.8	2.0
		ethene[d]	5.4	46	2.69	4.4	0.7	47	2.0
	473	vacuum	5.7	53	2.68	1.3	0.5	35	2.0
		ethene[d]	5.4	59	2.70	3.9	0.6	63	1.9
Pt/SiO_2-Al_2O_3	300	vacuum	6.1	32	2.68	2.3	0.3	−12	2.1
(1.46)		25 kPa ethene	5.5	31	2.70	4.2	1	59	1.9
	473	vacuum	5.9	45	2.68	1.6	0.3	3.5	2.1
		25 kPa ethene	5.9	51	2.72	4.8	0.4	−1.9	1.9
Pt/SiO_2-473	295	vacuum	5.1	8.4	2.70	0.0	0.1	−72	1.9
(1.21)	303	C_2H_4:H_2 = 1:3	6.7	2.4	2.76	0.7			
	373	C_2H_4:H_2 = 1:3	6.6	19	2.75	1.1			
	473	C_2H_4:H_2 = 1:3	6.9	50	2.77	−2	0.5	−6.3	2.1
Pt/SiO_2-873	300	vacuum	9.3	−13	2.75	−0.7			
(0.28)		33 kPa ethene	9.3	−13	2.76	−0.3			
	473	vacuum	9.4	7.7	2.75	−0.1			
		33 kPa ethene	9.2	11	2.75	−0.4			

[a] $3 < k < 13$ Å^{-1}, $1.6 < R < 3.1$ Å, including higher-order cumulants and with E_0, light scatterer = 0 eV.[32] [b] Platinum foil: $N = 12$, $\Delta\sigma^2 = 0$ Å^2, $R = 2.76$ Å, $\Delta E_0 = 0$ eV. [c] Errors: 15% in N, 100% in $\Delta\sigma^2$, 1% in R, and 2 eV in ΔE_0. [d] There was no difference between the structural parameters of the platinum clusters in pure ethene and in 25 kPa C_2H_4 with He as makeup gas.

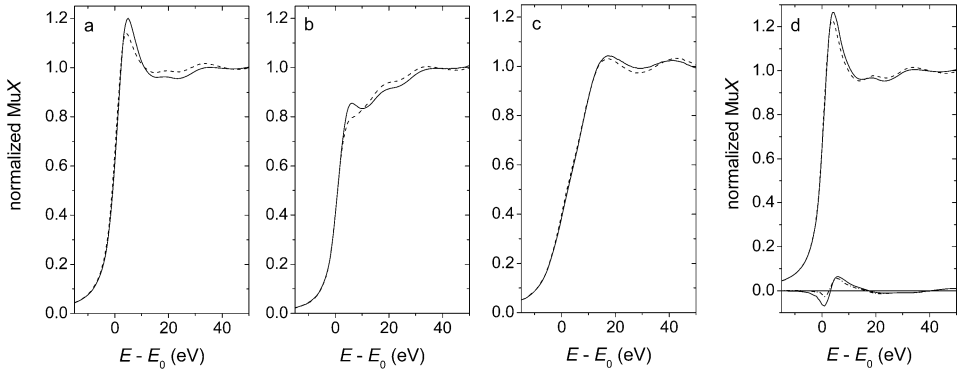

Figure 3. (a) Pt L_3 edge, (b) Pt L_2 edge, and (c) Pt L_1 edge for Pt/Al_2O_3 under vacuum at 300 K (---) and after admission of 25 kPa ethene in He at 77 K and heating to 300 K at 5 K/min (—). (d) Pt L_3 edge for $Pt/SiO_2-Al_2O_3$ under vacuum (---) and in 25 kPa C_2H_4 at 300 K (—), and the $\Delta\mu$ difference obtained from the spectrum in 25 kPa minus the spectrum under vacuum at 300 K (—) and 473 K (— · —).

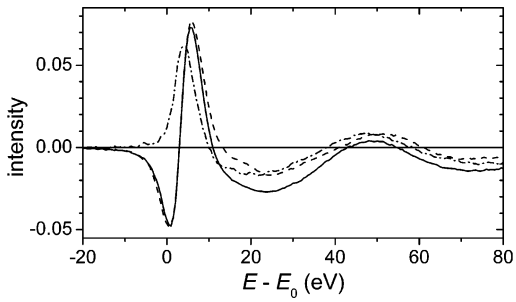

Figure 4. $\Delta\mu$ difference spectra (spectrum under vacuum at the same temperature as reference) at the Pt L_3 edge for Pt/Al_2O_3 in 25 kPa partial pressure of C_2H_4 at 77 K (— · —), and in pure ethene at 300 K (—) and 473 K (---).

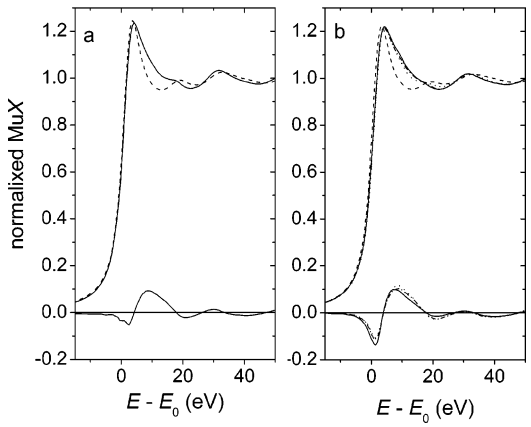

Figure 5. Pt L_3 edge for Pt/SiO_2 with small Pt clusters: (a) under vacuum (---), in 100 kPa H_2 at 300 K, and their difference (—), and (b) under vacuum (---), in 25 kPa C_2H_4/H_2 at 300 K (—), at 373 K (— · —), and at 473 K (···), and the corresponding $\Delta\mu$ difference with the spectrum under vacuum at the same temperature used as reference (same line patterns as the corresponding original spectrum).

in Figure 4. These ethene-induced changes are sharper and peak at lower energy than the H-induced changes at the L_3 edge (Figure 5a).[9,10,12,13] The ethene-induced effect at 77 K is a narrow intense peak at 5 eV and a negative feature at 25 eV. After heating the catalyst to 300 K, a larger negative contribution was observed around 0 eV, and an increase in intensity of the peak at 5 eV, which at its base was a bit broader than the spectrum measured at 77 K. The negative peak at 25 eV was more intense. The difference spectrum at 473 K resembled that at 300 K up to 5 eV; at higher energy the intensity was larger. All $\Delta\mu$ difference spectra featured a broad, shallow peak around

Table 2. Structural Parameters of Au/Al_2O_3 under Vacuum and in 20 mL/min 25 kPa C_2H_4 with Makeup Gas He As Determined by EXAFS Fitting of the Au L_3 Edges[a,b]

		Au–Au shell				Au–light scatterer shell		
			$\Delta\sigma^2$				$\Delta\sigma^2$	
T (K)	atmosphere	N[c]	(10^{-4} Å^2)	R (Å)	ΔE_0 (eV)	N	(10^{-4} Å^2)	R (Å)
300	vacuum	5.3	55	2.76	0.6	0.1	1.1	2.1
	ethene	6.2	76	2.75	3.1	0.1	1.1	2.1
373	vacuum	5.5	71	2.75	1.6	0.1	18	2.1
	ethene	5.6	70	2.76	2.0	0.1	−5.4	2.1
473	vacuum	5.3	84	2.75	1.3	0.1	28	2.1
	ethene	5.2	69	2.75	1.6	0.1	11	2.1

[a] $3 < k < 13$ Å^{-1}, $1.6 < R < 3.1$ Å, including higher-order cumulants and with E_0, light scatterer = 0 eV.[32] [b] Gold foil: $N = 12$, $\Delta\sigma^2 = 0$ Å^2, $R = 2.85$ Å, $\Delta E_0 = 0$ eV. [c] Errors: 15% in N, 100% in $\Delta\sigma^2$, 1% in R, and 2 eV in ΔE_0.

50 eV, with its intensity being lowest at 300 K. The L_3 $\Delta\mu$ difference for $Pt/SiO_2-Al_2O_3$ consisted of a small negative contribution at 0 eV, and a broad positive contribution from 3 to 16 eV (Figure 3d). At 473 K the negative contribution became more intense, and the intensity of the positive contribution increased slightly. The ethene-induced difference spectra for Pt/SiO_2-873 at 300 and 473 K were similar to that at 77 K for the smaller Pt clusters supported on Al_2O_3, but the intensity was twice as low.

The L_3 edges for Pt/SiO_2-473 upon chemisorption of hydrogen and upon admission of a gas mixture of ethene and hydrogen, in a 1:3 ratio, at 300 K are shown in Figure 5. The change in the L_3 edge upon admission of the gas mixture is clearly the same as the signature for hydrogen in an *n*-fold site. The increase in N_{Pt-Pt} and R_{Pt-Pt} and disappearance of the contribution of the light scatterer in the EXAFS are consistent with the chemisorption of hydrogen. The intensity of the $\Delta\mu$ difference spectrum decreased slightly when heating to 373 K, probably due to desorption of hydrogen. The shape changed upon further heating, and the contribution of the light scatterer appeared again in the EXAFS. Flowing 25 kPa ethene in hydrogen over Pt/Al_2O_3 with chemisorbed hydrogen also led to a Pt L_3 edge that resembled that of platinum with chemisorbed hydrogen. Apparently, since there was an excess of hydrogen, ethene was hydrogenated to ethane, and only hydrogen chemisorbed on the platinum surface. Ethene hydrogenation readily occurs on platinum at room temperature.[40]

Au/Al_2O_3. N_{Au-Au} of Au/Al_2O_3 was 5.3, corresponding to a cluster size of 0.8 nm (Table 2). The interatomic distance was 2.76 Å; thus, the Au−Au bonds were contracted by 0.09 Å with respect to the bulk value, as to be expected for clusters with such a low N_{Au-Au}.[41] Au−O scattering mimicking oxygen in the support at 2.1 Å was included in the fit. Upon addition of ethene at 300 K, N_{Au-Au} increased to 6.2, and it decreased again to the original value upon heating to 473 K. No significant carbon scattering from the adsorbed ethene was detected. Addition of ethene to the gold clusters caused significant changes in the Au L_3 and L_2 XANES (Figure 6); thus, ethene chemisorbs on the gold surface and induces changes in the electronic structure of gold. The ethene-induced change at 300 K was sharp and had a negative contribution above 10 eV (Figure 7). The $\Delta\mu$ resembled that for the Pt L_3 edge for Pt/Al_2O_3 at 77 K. At 373 K, the $\Delta\mu$ had the same shape, but a lower intensity. At 473 K, the $\Delta\mu$ was negative below 5 eV and broad with a low intensity at higher energy. The addition of ethene to Au/Al_2O_3 was done twice, at different beam lines, once in static mode and once in flow mode (shown here), and the same results were obtained in both experiments.

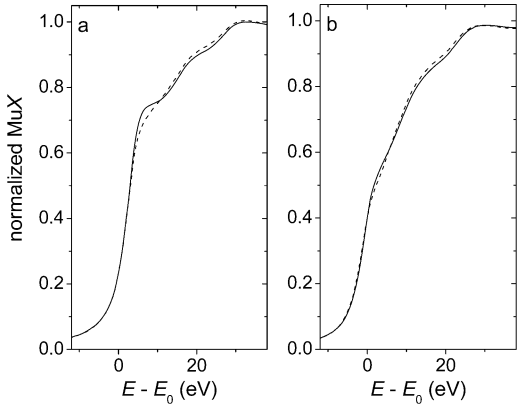

Figure 6. (a) Au L_3 edge and (b) Au L_2 edge for Au/Al_2O_3 under vacuum (---) and in 25 kPa C_2H_4 (—) at 300 K.

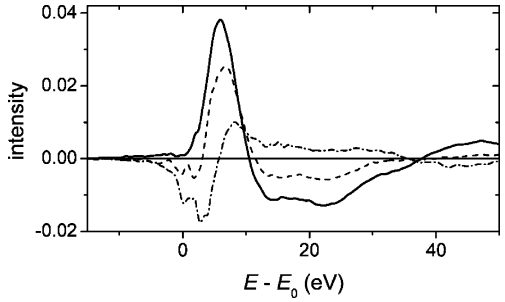

Figure 7. Difference spectra, $\Delta\mu$, at the Au L_3 edge for Au/Al_2O_3 in 25 kPa C_2H_4 at 300 K (—), at 373 K (---), and at 473 K (— · —) with respect to the spectrum under vacuum at the same temperature.

Table 3. Structural Parameters of $PtAu/SiO_2$ under Vacuum and in 25 kPa C_2H_4 in Helium As Determined by EXAFS Fitting of the Au and Pt L_3 Edges

		Pt–scatterer shell[a]				Au–scatterer shell[b]			
			$\Delta\sigma^2$				$\Delta\sigma^2$		
T (K)	atmosphere	N[c]	(10^{-4} Å^2)	R (Å)	ΔE_0 (eV)	N	(10^{-4} Å^2)	R (Å)	ΔE_0 (eV)
300	vacuum	9.0	35	2.76	1.6	7.4	−2.2	2.80	−2.1
	ethene	9.0	30	2.76	1.0	7.6	1.0	2.80	−1.4
473	vacuum	8.9	81	2.76	1.4	7.2	38	2.80	−1.9
	ethene	9.0	73	2.76	1.6	7.5	48	2.80	−1.4

[a] Pt L_3 EXAFS, $3.1 < k < 9$ Å^{-1}, $1.6 < R < 3.4$ Å, because of the short k range C_4 was not included. [b] Au L_3 EXAFS, $3 < k < 13$ Å^{-1}, $1.8 < R < 3.2$ Å, including higher-order cumulants.[32] [c] Errors: 15% in N, 100% in $\Delta\sigma^2$, 1% in R, and 2 eV in ΔE_0.

$PtAu/SiO_2$. The platinum atoms in $PtAu/SiO_2$ had 9 nearest neighbors, and the gold atoms had 7−8 neighbors (Table 3); thus, gold was preferentially located at the surface. The Pt−neighbor distance was 2.76 Å, indicative of gold and platinum neighbors, and the Au−neighbor distance was 2.80 Å. From electron microscopy, the metal cluster size was estimated to be ca. 1.5 nm. The structural parameters around both platinum and gold did not change upon admission of ethene; thus, the morphology of the PtAu clusters was not affected by ethene. Addition of ethene to the PtAu-alloy clusters induced a change in both the Pt and the Au L_3 XANES (Figure 8), suggesting that ethene adsorbs on both metals. The edges shifted to higher

(40) Somorjai, G. A.; Rupprechter, G. *J. Phys. Chem. B* **1999**, *103*, 1623.
(41) Miller, J. T.; Kropf, A. J.; Zha, Y.; Regalbuto, J. R.; Delannoy, L.; Louis, C.; Bus, E.; van Bokhoven, J. A. *J. Catal.* **2006**, *240*, 222.

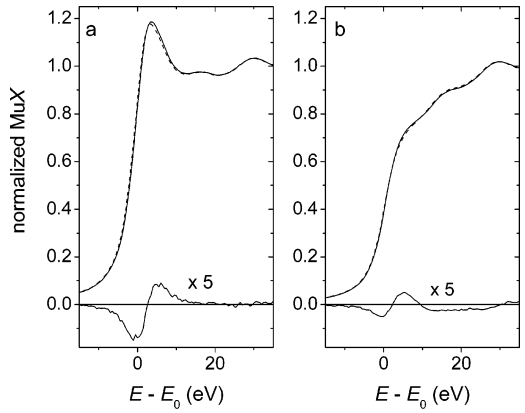

Figure 8. (a) Pt L_3 edge and (b) Au L_3 edge for $PtAu/SiO_2$ under vacuum (---) and in 25 kPa C_2H_4 (—) at 300 K, and their difference (—) multiplied by 5.

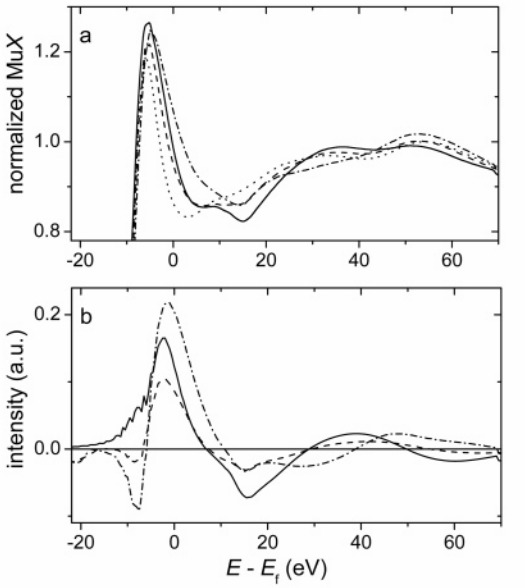

Figure 9. (a) FEFF8 calculated Pt L_3 edge for a Pt_6 cluster (···), and for Pt_6 with ethene adsorbed in the π-bonded (—), di-σ (---), or ethylidyne (— · —) mode. (b) FEFF8 calculated Pt L_3 $\Delta\mu$ signatures for ethene adsorbed on a Pt_6 cluster in the π-bonded (—), di-σ (---), and ethylidyne (— · —) modes.

energy. The $\Delta\mu$ difference spectra were similar for both metals, but the negative contribution was more intense for platinum. The $\Delta\mu$ magnitude at the Pt L_3 edge was twice as large as that at the Au edge, but smaller than the Pt L_3 $\Delta\mu$ for pure platinum clusters with similar coordination number (Figure 4).

Theoretically Predicted Signatures. Using the FEFF8 code, the XANES data for the bare Pt_6 and Au_6 clusters were calculated, as well as that for the clusters with ethene adsorbed in the π-bonded (Figure 1b), di-σ, and ethylidyne modes (Figure 1a). As shown in Figure 9a for the Pt_6 cluster, FEFF reproduces the XAS spectra of small platinum and gold clusters well in agreement with the literature.[13,16] The shape and intensity of the white line suggest that the platinum cluster has a three-dimensional structure,[19] which agrees with theoretical predictions.[42] Figure 9b shows the theoretically predicted $\Delta\mu$ difference spectra, or signatures, for different modes of ethene adsorption on a Pt_6 cluster. Although the Au−Au interatomic distances in the Au_6 cluster are slightly longer, the calculated $\Delta\mu$ signatures on gold are very similar and not shown here. The signature of π-bonded ethene has no negative contribution at low energy and a positive contribution around 0 eV. There is a broad peak at about 40 eV. The signature of di-σ bonded ethene is characterized by a small negative feature followed by a positive contribution of medium size. The broad peak is less pronounced than for π-bonded ethene and shifted to higher energy. The theoretical ethylidyne signature has a large negative contribution followed by an intense positive peak, which is broader than for π- and di-σ bonded ethene and has its maximum at about 0 eV. At about 20 eV a small feature is visible, and at about 45 eV there is a broad feature, which is at higher energies than for the other adsorption modes. Because the positions of the metal atoms in the cluster with and without ethene were unchanged, these signatures represent the changes induced by the adsorbed species. As indicated by the EXAFS analyses of the experimental data, the metal−metal distances and coordination numbers did not change significantly after ethene adsorption; thus, the FEFF8 predicted signatures can be directly compared to the experimental ones. The theoretical signatures reflect the changes in the XANES of a unique adsorbate on the metal surface, whereas the changes in the experimental spectra could be caused by a multiple of species. Because XAS measures an averaged signal of all atoms in a sample, the signature of all species will be superimposed. The most-present species will dominate the signal, and minor species likely remain undetected. We estimate that species that are present in concentrations below 15% may remain undetected. As will be shown, the signature of mixed adsorbates consisting of hydrogen and ethylidine can be distinguished, because of their presence in equal amounts. Improvements in experimental techniques that enhance the spectral resolution will provide more spectral detail and improve the accuracy.

Discussion

Electronic Effect on Platinum. The addition of ethene to the platinum catalysts induced changes in the Pt L_3 white line, indicating changes in the electronic structure that result from the bonding of ethene to the metal. Upon bonding of reactants such as ethene and CO to a metal surface, bonding and antibonding states are formed. Electrons are transferred from the π orbitals of the adsorbate to the unoccupied d orbitals of the metal, and a back-donation populates the ethene or CO π^* orbitals with electrons from the occupied metal orbitals.[43−45] The resulting empty antibonding states of d character are observed in the white line of the L_3 edge, which probes the number of holes in the d band. All of these effects are incorporated into the FEFF8 code that accounts for the $\Delta\mu$, and these effects depend on the adsorbate site, producing the different $\Delta\mu$ signatures. Infrared spectroscopy, in contrast, probes the changes in the C═C and CO stretch frequencies that are due to the charge donation of the metal to the adsorbates. An increase in the white-line intensity due to the withdrawal of electron density from small platinum clusters by adsorbed ethene has been observed before; however, the spectra were not shown or interpreted.[4]

(42) Wang, L. L.; Johnson, D. D. *J. Am. Chem. Soc.* **2007**, *129*, 3658.
(43) Chatt, J.; Duncanson, L. A. *J. Chem. Soc.* **1953**, 2939.
(44) Duddell, D. A. *Spectrosc. Struct. Mol. Complexes* **1973**, 387.
(45) Blyholder, G. *J. Phys. Chem.* **1964**, *68*, 2772.

Table 4. Ethene Adsorption Modes under Various Conditions

sample	cluster size (nm)	atmosphere	adsorption site temperature <100 K	300 K	373 K	473 K
Pt/Al_2O_3	0.8[a]	25 kPa C_2H_4	π (and di-σ)	ethylidyne		dehydrogenated ethene + H
Pt/Al_2O_3	0.8	100 kPa C_2H_4		ethylidyne		dehydrogenated ethene + H
Pt/SiO_2-Al_2O_3	0.8	25 kPa C_2H_4		ethylidyne + H		dehydrogenated ethene + H
Pt/SiO_2	*0.6*	*25 kPa* C_2H_4 + 75 kPa H_2		H in *n*-fold site	H in *n*-fold site	H in *n*-fold site
Pt/SiO_2	3	33 kPa C_2H_4		π and di-σ		π and di-σ
Pt	single crystal[b]	10^{-4} Pa C_2H_4	π	di-σ and ethylidyne	ethylidyne	ethylidyne + H
Au/Al_2O_3	0.7	25 kPa C_2H_4		π and di-σ	π and di-σ	
$PtAu/SiO_2$	1.5	25 kPa C_2H_4	low coverage in *n*-fold sites consisting of Pt and Au			

[a] For the smallest clusters, an expected range of ±0.3 nm can be assumed. [b] From ref 3.

Adsorption Sites. The $\Delta\mu$ difference spectra (referenced to bare metal clusters) showed characteristic variations with temperature and pressure, and moreover, these variations differed from those after hydrogen chemisorption. By comparing the experimental $\Delta\mu$ to the theoretically predicted ones, the adsorption sites can be determined as a function of temperature and composition of the gas phase. Table 4 gives an overview of the determined adsorption modes under various conditions for the different catalysts. The ethene-induced change in the Pt L_3 edge of Pt/Al_2O_3 at 77 K resembles the predicted π-bonded signature, or a mixture of π- and di-σ bonded ethene on sites consisting of one or two platinum atoms (cf. Figures 4 and 9). There is a negative contribution at low energy in $\Delta\mu$ at 300 K, and the broad component at about 50 eV is lower than at 77 K. These characteristics indicate a conversion to an ethylidyne species in a threefold Pt site. The broadening of the feature at 10 eV upon further heating indicates that hydrogen is coadsorbed. The ethene-induced change in the L_3 XANES of $Pt/SiO_2-Al_2O_3$ at 300 K is broader than that for Pt/Al_2O_3 and can be interpreted as adsorbed ethylidyne plus hydrogen (Figure 3d). Mixed adsorbates on a cluster can be detected by the $\Delta\mu$ approach; however, because of the overlapping signatures, agreement with the FEFF8 single adsorbate results become less quantitative. Upon heating, the first feature in $\Delta\mu$ becomes more negative, and the positive contribution broadens, indicating more chemisorbed H, thus further dehydrogenation. The dehydrogenation of ethene proceeds at lower temperature on small $SiO_2-Al_2O_3$-supported platinum clusters than on Al_2O_3-supported clusters. In a gas mixture of ethene and hydrogen, the Pt L_3 $\Delta\mu$ resembles the signature of a surface fully covered with hydrogen in *n*-fold sites (Figure 5). All ethene is hydrogenated to ethane, and hydrogen then preferentially adsorbs on the platinum surface.[46,47]

The transition from weakly bonded π- and di-σ adsorbed ethene at low temperature, to ethylidyne species and dehydrogenation at higher temperature, is expected. With sum-frequency generated infrared spectroscopy, NEXAFS, and XPS, it was found that on platinum single crystals the adsorption mode is π below ca. 100 K. The π-bonded ethene is converted to di-σ bonded ethene between 100 and 250 K, and to ethylidyne between 250 and 300 K.[3,40,48−51] We showed that on small platinum clusters ethene already adsorbs in the di-σ mode in addition to the π-bonded mode at 77 K, and ethylidyne is formed already at temperatures below 300 K. On the large platinum clusters on SiO_2 used in this study, the adsorption sites are on-top and bridged, both at 300 and 473 K. Thus, activation of ethene on small clusters occurs at lower temperatures than on single crystals and larger clusters, in agreement with the increase in the turnover rates for C−H bond activation with decreasing cluster size.[52] Small metal clusters have more edges and corners that are more reactive. Although the equilibrium shifts toward the more weakly bonded species at the high coverages and pressures used here,[3] the higher reactivity of the small clusters makes up for the coverage/pressure effect. Others found that on Pt/SiO_2 ethene adsorbs in the π- and di-σ bonded mode below 189 K and that some of the di-σ bonded species were converted to ethylidyne when heating to room temperature, or that the main surface species on Pt/SiO_2 at 300 K was ethylidyne, but the Pt cluster sizes were not given in these studies.[53,54] This comparison with results obtained from other techniques shows that in situ XANES on the L_3 edge is highly suitable for the determination of the adsorption sites of ethene under catalytically relevant conditions.

Application to Gold and Alloy Catalysts. We have shown before that the electronic structure of small gold clusters supported on Al_2O_3 changes upon addition of hydrogen,[34] and we show here that ethene also induces changes in the gold electronic structure. This proves that hydrogen and ethene form bonds with the gold nanoclusters, in agreement with their activity in hydrogenation reactions.[23] Comparison of the Au L_3 $\Delta\mu$ for Au/Al_2O_3 with the theoretically predicted signatures shows that the ethene adsorption site on small gold clusters is both on-top and bridged at 300 K (Figure 7). On small platinum clusters of similar size, ethylidyne species are adsorbed at 300 K. In the π and di-σ adsorption modes, in which one ethene molecule adsorbs on one or two metal atoms, the metal−ethene interaction is weaker than in the ethylidyne mode, in which ethene adsorbs in a threefold metal site. Thus, the interaction of gold with ethene is weaker than the Pt−ethene interaction, consistent with the lower activity of gold compared to platinum. On Au single crystals the adsorption energy of ethene in the π and di-σ modes is calculated to be between −0.15 and −0.78

(46) Stuck, A.; Wartnaby, C. E.; Yeo, Y. Y.; King, D. A. *Phys. Rev. Lett.* **1995**, *74*, 578.
(47) Watwe, R. M.; Spiewak, B. E.; Cortright, R. D.; Dumesic, J. A. *J. Catal.* **1998**, *180*, 184.
(48) Hatzikos, G. H.; Masel, R. I. *Surf. Sci.* **1987**, *185*, 479.
(49) Yagasaki, E.; Backman, A. L.; Masel, R. I. *J. Phys. Chem.* **1990**, *94*, 1066.
(50) Horsley, J. A.; Stöhr, J.; Koestner, R. J. *J. Chem. Phys.* **1985**, *83*, 3146.
(51) Lee, A. F.; Wilson, K. *J. Vac. Sci. Technol., A* **2003**, *21*, 563.
(52) Ramallo-López, J. M.; Requejo, F. G.; Craievich, A. F.; Wei, J.; Avalos-Borja, M.; Iglesia, E. *J. Mol. Catal. A: Chem.* **2005**, *228*, 299.
(53) De la Cruz, C.; Sheppard, N. *J. Chem. Soc., Faraday Trans.* **1997**, *93*, 3569.
(54) Shen, J.; Hill, J. M.; Watwe, R. M.; Spiewak, B. E.; Dumesic, J. A. *J. Phys. Chem. B* **1999**, *103*, 3923.

eV, whereas on Pt(110)-(1 × 2) it is −1.48 eV in the di-σ mode.[55,56] At 373 K the gold adsorption site is evidently bridged, but the ethene-induced XANES difference spectrum at 473 K does not resemble any of the theoretical signatures. The change is characterized by a broad positive contribution from 7 to 35 eV. On a mononuclear supported Au(III) complex the ethene adsorption mode was π, as found with infrared spectroscopy.[57] EELS and static secondary-ion mass spectroscopy studies showed that ethene adsorbed in the π mode on <1 ML Au on Ru(1000) at 130 K and in temperature-programmed studies ethene adsorbed molecularly on Au(110) and desorbed between 100 and 200 K.[58,59] The supported gold clusters still interact with ethene at 373 K, since the clusters have a higher reactivity than bulk Au, because of their narrower d band that lies closer to the Fermi level.[60,61,64]

The in situ XAS experiments show that ethene adsorbs on both platinum and gold in bimetallic clusters, and thus that gold cannot be considered as just an inactive additive. This shows the advantage of probing the structure at both metal edges instead of just the adsorbate as in vibrational spectroscopy. On the PtAu-alloy clusters, the intensity of $\Delta\mu$ is lower than those on the monometallic platinum and gold clusters, indicating that on a per atom basis less ethene is adsorbed (Figure 8). The low intensity of the ethene-induced change is due to the low surface concentration of platinum.[62] Although the difference spectra cannot unambiguously be assigned to a certain ethene or hydrogen adsorption site, the shifts of the Pt and Au L_3 edges to higher energy indicate that the adsorption site is two- or threefold. Thus, ethene is proposed to adsorb in threefold hollow and bridged sites that involve both platinum and gold atoms. In contrast, from TPD experiments with supported AuPd model catalysts it was concluded that addition of gold leads to a decrease in the amount of di-σ bonded ethene requiring adjacent palladium atoms.[63]

Structural Changes. Although there are structural changes in the platinum clusters upon hydrogen chemisorption, as indicated by the systematic higher coordination numbers and longer Pt−Pt distances in hydrogen relative to vacuum, we observed no significant changes in the geometric structures of the supported noble metal clusters due to ethene adsorption. In contrast, restructuring of single-crystal metal surfaces has been reported upon adsorption of reactants. For example, the metal atoms of Pt or Rh(111) single crystals break away from corner or edge sites in the presence of CO to form multiple-bonded CO metal complexes.[40] As observed for $Pt/SiO_2-Al_2O_3$ and Pt/Al_2O_3, the coadsorbed hydrogen, which is formed upon dehydrogenation, leads to a relaxation of the contracted Pt−Pt distance. The increase in R_{Pt-Pt} upon H chemisorption is explained by the electron-withdrawing properties of hydrogen: the decrease in electron density between the platinum atoms lengthens the interatomic distance.[39] Upon ethene adsorption electrons are transferred from the π orbitals of ethene to the unoccupied d orbitals of platinum and back from the occupied metal orbitals to the ethene π^* orbitals.[43−45] The net charge transfer is less than in the case of H chemisorption, and therefore has no significant effect on R_{Pt-Pt} and the structure of the platinum clusters. Gates et al. found a modification of both the electronic and structural properties of platinum clusters exposed to alkenes, using in situ XAS.[4,5] For platinum clusters of 1.1 nm, they determined an R_{Pt-Pt} of 2.70 Å under vacuum, which increased to 2.76 Å in hydrogen, and decreased again to 2.71 Å when switching to an ethene flow, at 298 K and atmospheric pressure. The N_{Pt-Pt} decreased from 6.5 in hydrogen to 4.1 in ethene, and the Debye−Waller factor increased. The structural changes were reversible. Platinum clusters of 2.1 nm showed much smaller structural changes. These changes in the structural parameters concur with our observation that the coordination number in hydrogen is higher than in ethene atmosphere and vacuum, especially for the smallest platinum clusters. These authors did not identify Pt−C contributions, because of difficulties in the separation of these contributions from the Pt−$O_{support}$ contributions that were characterized by large Debye−Waller factors.[4] Our data suggest that there is a small Pt−C contribution caused by ethene adsorption, determined by fitting carbon and oxygen as one shell, and taking the difference between the coordination number before and after ethene adsorption, and by analysis of the EXAFS difference spectra.

Conclusions

The changes in the electronic structure of the empty valence d band of metals caused by the bonding of adsorbates are detected in the L_3 and L_2 X-ray absorption near-edge spectra. These changes reflect the adsorption sites of the adsorbates. Difference spectra, $\Delta\mu$, are especially sensitive to the changes in the electronic and geometric structures that occur after the adsorption of reactants and intermediates. We showed that comparison of these difference spectra to theoretically predicted difference spectra reveals the specific adsorption of hydrocarbon molecules under catalytic reaction conditions, thus enabling the determination of the sites that participate in catalytic reactions. This delta XANES analysis provides complementary information to the EXAFS analysis and to vibrational spectroscopies. Application of this technique to supported platinum, gold, and PtAu-alloy clusters showed that the electronic structure of these clusters changed upon addition of ethene. Analysis of the difference spectra revealed that ethene is π and di-σ bonded on small platinum clusters at 77 K and atmospheric pressure. Below 300 K ethene is converted to ethylidyne species and hydrogen, which both occupy *n*-fold sites on the platinum clusters. The dehydrogenation is faster on $Pt/SiO_2-Al_2O_3$ compared to Al_2O_3-supported clusters. Geometrical changes to the clusters do not occur upon admission of ethene; rather, the Pt−Pt coordination number and distance increase upon chemisorption of hydrogen that is formed in the dehydrogenation of ethene. Bulklike platinum clusters are less reactive, and consequently, the ethene−metal interaction is weaker and the dehydrogenation proceeds at higher temperature, as for platinum single crystals. In a reaction mixture of ethene and hydrogen there is primarily hydrogen chemisorbed on the Pt surface. Ethene adsorbs on small supported gold clusters, and their reactivity is lower compared to small platinum clusters. Furthermore, ethene adsorbs on both platinum and gold in the bimetallic clusters,

(55) Zinola, C. F.; Castro Luna, A. M. *J. Electroanal. Chem.* **1998**, *456*, 37.
(56) Loffreda, D. *Surf. Sci.* **2006**, *600*, 2103.
(57) Guzman, J.; Gates, B. C. *J. Catal.* **2004**, *226*, 111.
(58) Sakakini, B.; Swift, A. J.; Vickerman, J. C.; Harendt, C.; Christmann, K. *J. Chem. Soc., Farad. Trans. 1* **1987**, *83*, 1975.
(59) Outka, D. A.; Madix, R. J. *J. Am. Chem. Soc.* **1987**, *109*, 1708.
(60) Lopez, N.; Nørskov, J. K. *J. Am. Chem. Soc* **2002**, *124*, 11262.
(61) Jain, P. K. *Struct. Chem.* **2005**, *16*, 421.
(62) Bus, E.; van Bokhoven, J. A. Submitted.
(63) Luo, K.; Wei, T.; Yi, C.-W.; Axnanda, S.; Goodman, D. W. *J. Phys. Chem. B* **2005**, *109*, 23517.
(64) Bus, E.; van Bokhoven, J. A. *J. Phys. Chem. C* **2007**, in press.

illustrating the advantage of studying the structure of the metal under catalytic conditions.

Acknowledgment. The authors thank J. T. Miller for the synthesis of Pt/SiO_2 and $Pt/SiO_2-Al_2O_3$, T. M. Schmid for help with the $Pt_2Au_4(C{\equiv}CBu^t)_8$ synthesis, Hasylab (Hamburg, Germany) and the European Synchrotron Radiation Facility (Grenoble, France) for provision of synchrotron radiation facilities, and the staff of Station X1 at Hasylab (I-04-087) and the Dutch-Belgian Beam line (CH-2129) at the ESRF for their support. The work at Hasylab was supported by the European Community—Research Infrastructure Action under the FP6 "Structuring the European Research Area" Program, Contract RII3-CT-2004-506008. J.A.v.B. thanks the Swiss National Fonds for financial support.

JA0689233